Volume 6, Issue 1, 2016, 1053-1058 ISSN 2069-5837

Biointerface Research in Applied Chemistry

www.BiointerfaceResearch.com

Original Research Article Open Access Journal

Received: 21.01.2016 / Revised: 10.02.2016 / Accepted: 12.02.2016 / Published on-line: 13.02.2016

Ag-nanoparticle-based nano-immunosensor for anti-glutathione S-transferase detection

Akemi Martins Higa [1], Giovanni Pimenta Mambrini [1], Moema Hausen [1], Francisco Trivinho Strixino[1], Fábio de Lima Leite [1,*]

[1]Department of Chemistry, Physics, and Mathematics, Federal University of São Carlos, Sorocaba, São Paulo, Brazil.

*corresponding author e-mail address: ***fabioleite@ufscar.br***

ABSTRACT

The purpose of this research was to study the synthesis of Ag nanoparticles (AgNPs) and their functionalization via conjugation with the protein glutathione S-transferase (GST) to introduce interfacial properties for the specific biosensing of the antibody anti-glutathione S-transferase (anti-GST). This study was conducted in order to investigate the efficiency of the AgNPs at detecting specific antibodies in immunoassays. In this paper, we report the synthesis of AgNPs with a chemical reduction method, which consists in the reduction of silver nitrate with sodium citrate. The GST-functionalized AgNPs were obtained by incubating the AgNP suspension in a GST-containing solution. The functionalization process was characterized via colorimetric detection and characterization techniques, such as Fourier-Transform Infrared (FT-IR) Spectroscopy and Laser Scanning Confocal Microscopy (LSCM). The activity of the nano-immunosensor was monitored via spectrophotometric techniques, which showed that anti-GST was detected by the AgNP-GST complexes. The spectrophotometric techniques also allowed us to monitor the room-temperature suspension stability of the nano-immunosensor. The results of this study show the potential of the GST-functionalized AgNPs for the detection of specific antibodies because of their suitable optical properties and high sensitivity for various anti-GST concentrations.

Keywords: *Ag nanoparticles, nano-immunosensors, glutathione S-transferase, anti-glutathione S-transferase, chemical reduction method.*

1. INTRODUCTION

According to the literature, there are many studies related to the application of metal nanoparticles (MNPs) for detecting specific biomolecules in colorimetric assays because of the photochemical properties of nanoscale noble metals, which favour the development of biosensor devices[1,2]. The specific functionality of MNPs is accomplished via various surface modifications with functional molecules[3].

In the present study, we investigated the functionalization of Ag nanoparticles (AgNPs) with the antigen glutathione S-transferase (GST) to evaluate the efficiency of the AgNPs as an analytical device for the detection of anti-glutathione S-transferase (anti-GST) in specific immunoassays. The GST protein catalyses the nucleophilic attack of glutathione (GSH) on non-polar compounds that contain an electrophilic C, N, or S atom. This protein has both pharmacological and toxicological significance in the metabolism of carcinogens and chemotherapeutic agents in tumours and asthma treatments. It also catalyses reactions involving the metabolism of herbicides and insecticides in plants[4].In our study, the fabricated AgNPs had a particle-size distribution (2−10 nm) that is similar to that of semiconductor nanocrystals, *i.e.* quantum dots (QDs)[5]. With such dimensions, the photochemical properties of the AgNPs can be tuned by adjusting their composition or size[6].

Thus, the optical emission and absorption spectra of the nanoparticles are dependent on their size and shape[7]. This means the AgNPs have several advantages over organic fluorophore dyes, such as broad emission and absorption bands. Therefore, the AgNPs have a broad excitation spectrum and clearly defined emission peaks, both of which ensure the generation of signals that exhibit minimal spectral interference between the AgNPs and natural fluorescence of the biomolecules[1]. In addition, the colloidal stability of the AgNPs after repeated cycles of excitation and fluorescence is noteworthy. The stability can be optimized via functionalization because the attached molecules minimize the agglomeration of the AgNPs[8].

In the presence of target proteins, the functionalized AgNPs exhibited a high sensitivity towards the specific analyte present in the solution. The intermolecular reactions between the functionalized AgNPs and specific analyte were detected via optical signals, *i.e.* the changing colour of the AgNP suspension and variation in the corresponding fluorescence intensity. These changes are caused by the alterations made to the surface of the functionalized AgNPs, which are generated by the non-covalent antibody-antigen bonding[6].

AgNPs were chosen for the development of the nano-immunosensor because of their low toxicity, low-cost synthesis, high colloidal stability, and as mentioned above, excellent photochemical properties that are associated with biological compatibility[9]. These are the main advantages of using AgNPs over QDs, which have a high toxicity, low suspension stability, and high-cost processing and experimental manipulation[10].

Therefore, studying the chemical properties and surface functionalization of AgNPs is relevant to the biotechnological field regarding the construction of nanodevices that can be incorporated into goodclinical laboratory practices. The few papers published on this subject have shown that the application of AgNPs in studies focused on the detection of specific biomolecules have had promising results. Thus, such research has

the potential to contribute to the progress of diagnostic immunopathology[1, 11].

In a study of the cancer biomarker and antigen alpha-fetoprotein (AFP) by Tang *et al.*[11], it was shown that AFP has a high affinity for immobilized anti-AFP antibodies on the surface of AgNPs. Dawan *et al.*[12] modified electrodes with AgNPs functionalized with specific antibodies, such as anti-human serum albumin (anti-HSA), anti-penicillin G (anti-PenG), and anti-microcystin-LR (anti-MCLR), to evaluate the sensitivity and detection limit of the AgNPs towards the corresponding antigens. They demonstrated that the electrodes modified with AgNPs have an enhanced sensitivity and detection limit compared to other sensors. Chen *et al.*[13] functionalized AgNPs with streptavidin (SA) via electrostatic interactions for the detection of biotinylated aptamers in cell culture media. The aptamers labelled with biotin were detected by the SA-functionalized AgNPs, and therefore, exhibited potential as biocompatible probes for cell culture media.

Naja *et al.*[14] functionalized AgNPs with Protein A for conjugation with anti-*Escherichia coli* (anti-*E. coli*) antibodies. To demonstrate the selectivity of the functionalized AgNPs, the authors conducted two detection assays: a specific assay with *E. coli* cells and a non-specific assay with *Rhodococcus rhodochrous* (*R. rhodochrous*) cells. By employing Raman spectroscopy, the authors demonstrated that *R. rhodochrous* was not adsorbed onto the surface of the anti-*E.coli*-functionalized AgNPs.

The purpose of our study was to synthesize and functionalize AgNPs for the detection of anti-GST via surface modifications with GST. Thus, we investigated the interactions between the AgNP-GST complexes and anti-GST to determine the efficiency of the chromophores when applied to antibody detection.

2. EXPERIMENTAL SECTION

2.1. Synthesis and Functionalization of AgNPs.

The method applied in this study was based on the Turkevich method, which does not use toxic substances and generates minimal residue. The AgNP suspension was prepared chemically via the reduction of silver nitrate ($AgNO_3$ – ≥99%, Synth®) with sodium citrate (trisodium citrate, $Na_3C_6H_5O_7$ – ≥99%, Synth®)[15]. All solutions were prepared with deionized water, and all chemicals were used as received. In brief, 100 mL of an aqueous solution of $AgNO_3$ (1.0 mmol/L) was heated to 90 °C. Then, 1 mL of an aqueous solution of sodium citrate (0.3 mol/L) was added to promote the reduction of $AgNO_3$. The precipitation of AgNPs with a radius of approximately 5 nm was indicated by the colour of the suspension changing from clear to yellow as the sodium citrate was added, as reported in the literature[15]. The functionalization of the AgNPs was achieved by adapting the method presented by Marangoni *et al.*[16]. In their study, they functionalized AuNPs with jacalin (a protein). Their synthetic method consisted of adding the jacalin-containing solution to the AuNP suspension and maintaining the mixture at 4 °C for 24 h[16].

2.2. Characterization of the AgNPs.

Fourier transform infrared (FT-IR) spectroscopy (Thermo Scientific Nicolet™ IR200) in the attenuated total reflectance (ATR) mode was used to verify the presence of the different substances on the surface of the functionalized AgNPs by comparing the distinct spectral signatures of the analysed films. The spectra were collected at a spectral resolution of 4 cm^{-1}, with 256 scans performed over 2500–400 cm^{-1}. For the FT-IR analysis, the suspensions were dried on single-crystal Si substrates to decrease the intensity of the signals caused by the presence of water.

Laser scanning confocal microscopy (LSCM) (Leica Microsystems CMS GmbH)was used to observe the fluorescence of the non-functionalized AgNPs (hereinafter referred to as free AgNPs) and GST-functionalized AgNPs, and to create reconstructed 3D images of the samples. An aliquot of the free or functionalized AgNPs (1 ng/mL) was deposited on a glass slide and observed with LSCM. The images of the free and functionalized AgNPs were acquired via LAS AF software (Leica Microsystems CMS GmbH) in the photomultiplier tube (PMT) mode; 10% of the 488 nm laser line and 5% of the 638 nm laser line were used to create the images. The images were captured in the spectral band where the samples exhibited the highest fluorescence intensity, *i.e.* 485–570 nm for free AgNPs and 580–700 nm for the GST-functionalized AgNPs. To capture the control images, *i.e.* those for which no or minimal fluorescence intensity was detected, the laser lines used were 5% of the 405-nm UV diode (spectral region = 380–440 nm) for the free AgNPs and the 638 nm laser line (spectral region = 720–780 nm) for the GST-functionalized AgNPs. The 3D reconstruction was achieved by overlapping 30 optical sections. All of the analyses were performed in duplicate.

2.3. Antibody detection of the nano-immunosensor.

The immunoassays were prepared by diluting an anti-GST-containing solution with the GST-functionalized AgNP suspension. The absorbance of the suspension was measured with a spectrophotometer (Shimadzu UV-3600 UV-Vis-NIR) in the visible region of the electromagnetic spectrum (580 nm). Six dilutions (1:500, 1:1000, 1:2000, 1:4000, 1:8000, and 1:16000) of the anti-GST stock solution (1000 ng/mL) were prepared in phosphate-buffered saline (PBS) with a pH of 7.2. The concentration of GST, which was attached to the surface of the AgNPs, was maintained at 1000 ng/mL. The absorbance spectra were measured for each dilution at regular intervals. The first reading was performed immediately after mixing the solutions. After 10 min, the absorbance of the mixture was measured. The absorbance was then measured every 10 min until 60 min had passed.

3. RESULTS SECTION

When synthesizing the AgNPs, the reaction time and temperature determine their size. According to JI *et al*. [17], larger NPs are obtained with longer reaction times and higher temperatures. Controlling the size of the AgNPs is crucial as it determines the chemical and physical properties of the NPs[18]. In our study, the reaction time and temperature used were 12 min and 90 °C, respectively, which are the parameters used in the work of Gorup *et al*.[15]. According to these conditions, the resulting AgNPs should have a radius of 5 nm, as evidenced by the formation of a homogeneous yellow suspension. The chemical reduction of a metal salt is a simple synthetic route and generates an AgNP suspension that is stabilized by citrate.

The effective functionalization of the as-prepared AgNPs is required for the detection of anti-GST. The functionalization process must ensure the suspension stability and maintain the structural integrity of the biomolecules to preserve the catalytic activity of the functional groups. GST has four highly reactive cysteine residues[19] that enable the bonding of the biomolecule to the surface of the AgNPs[20]. Cysteine is an amino acid that contains a thiol group (-SH), which is involved in the catalytic activity of the protein, and consequently, in its physiological processes. In addition, it determines the affinity of the protein for heavy metals[21].

FT-IR spectroscopy was employed to characterize the chemical reactions that lead to the formation of the bioconjugates via the functionalization process. The FT-IR spectra of five films (GST (1000 ng/mL), anti-GST (1000 ng/mL), the free AgNPs, the GST-functionalized AgNPs, and the immunoassay containing the functionalized AgNPs and anti-GST were measured, with the results shown in (Figure 1).

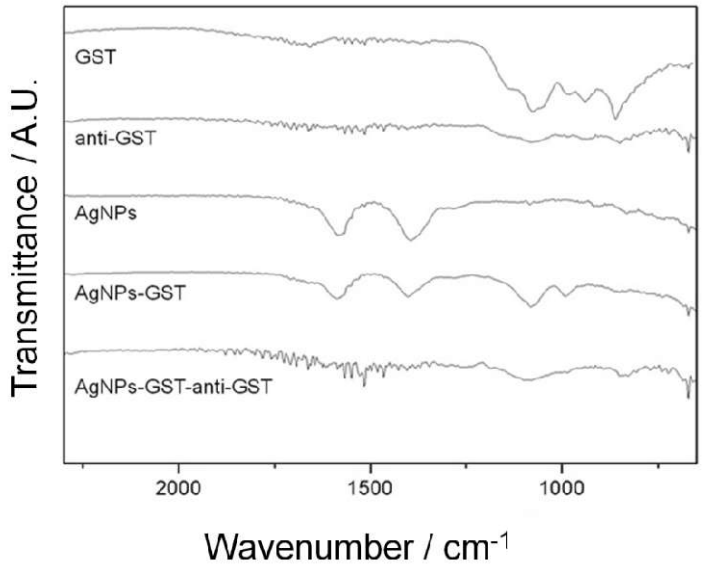

Figure 1. FT-IR spectra of the films formed by drying the different suspensions.

The spectral signature of GST appears in the spectral region between 1250 and 750 cm^{-1}, while that of anti-GST appears between 2000 and 750 cm^{-1}. In addition, the two characteristic peaks of the free AgNPs appear between 1750 and 1250 cm^{-1}. These spectral signatures are present in the spectra of the films formed from the pure solutions, and are used as references to confirm the effectiveness of the functionalization process. A combination of the AgNP and pure GST spectral signatures is present in the spectrum of the GST-functionalized AgNPs. In the FT-IR spectrum of the immunoassay film, there is evidence of the GST, anti-GST, and AgNP spectral signatures. The last two spectra in (Figure 1) indicate the presence of complexes that are the result of intermolecular interactions between the AgNPs and the biomolecules because there is a mixture of the spectral signatures of the pure solutions and not just a summing of them, which would only indicate the presence of different molecular groups and not the interactions between them[22].

The topographic characterization of the free and functionalized AgNPs (Figures 2A and C, respectively) was performed with LSCM. The images were obtained via optical sections, which were then superimposed over the surface of the sample to create a topographic reconstruction[23]. In addition, it is possible to set the laser lines to detect the emission of fluorescent signals between 350 and 800 nm, as well as analyse the fluorescence intensity.

The AgNPs emit intense fluorescence from 500 nm and above, and therefore, a range of 485 to 570 nm was used to identify them (Figure 2A). To verify that the emitted fluorescence was caused by the presence of the AgNPs, control images were taken of the same sample area in the range of 380–440 nm, which did not exhibit a fluorescence signal (Figure 2B)[24]. The most intense GST fluorescence signal was observed in the range of 580–700 nm (Figure 2C). The wide excitation band and fluorescence emission of the AgNPs means that the fluorescence signals of the AgNPs and biomolecules overlap[1].

To exclude the possibility of detecting a non-GST-related emission, a control image was captured in the spectral range of 720–780 nm (Figure 2D). In this spectral range, an intense fluorescence signal caused by the AgNPs is still present, and virtually no fluorescence signal from the GST can be seen when comparing Figures 2C and D. In addition, regions of interest (ROIs) were selected and are indicated by the orange, green, and purple lines in (Figure 2). These regions were selected because of the overlapping fluorescence signals of both the AgNPs and GST at 580 nm, which would allow us to determine the different fluorescence intensities corresponding to the AgNPs and GST for evidence of their co-location. The ROIs represented by the lines 1, 2, and 3 refer to the first parameters used in the experiments, *i.e.* the spectral bands in which the highest fluorescence intensities were observed for the AgNPs (485–570 nm) and GST (580–700 nm). By excluding certain wavelengths, it was possible to evaluate the co-location of the AgNPs and GST by capturing images in two pseudo-colours and the signal intensities produced by the AgNPs and GST. As the AgNPs emit fluorescence in the visible region of the spectrum above 500 nm, the pseudo-colour term is used here because the colour of each sample (red for the functionalized AgNPs and blue for the free AgNPs) was chosen by the user to facilitate the separation of the spectra of each sample. The plots of fluorescence intensity as a function of position that were generated from these measurements can be used to establish the relative positions of the AgNPs and GST, which is important for evaluating the effectiveness of the functionalization process[25].

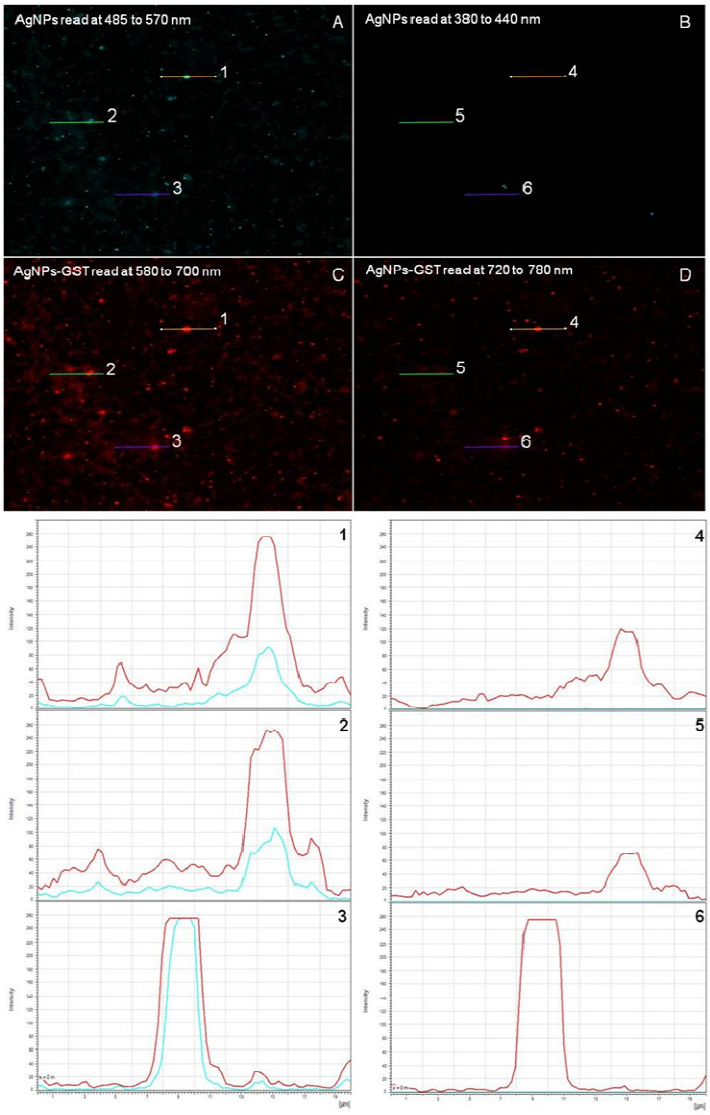

Figure 2. LSCM images of the free and functionalized AgNPs. (A) The maximum fluorescence signal of the free AgNPs (485–570 nm). (B) The absence of the fluorescence signal of the free AgNPs (380–440 nm). (C) The maximum fluorescence signal of GST (580–700 nm). (D) The absence and presence of the GST and AgNPs fluorescence signals, respectively (720–780 nm). (Plots 1–Plots of fluorescence intensity as a function of position for the ROIs indicated in Fig. 2A by the three coloured lines that are 20 μm in length: 1 = orange, 2 = green, and 3 = purple. In plots 1, 2, and 3, the red lines represent the intensity of the GST fluorescence and the blue lines represent the intensity of the AgNP fluorescence. In plots 4, 5, and 6, the red lines represent the intensity of the fluorescence emitted in Fig. 2D because there was no fluorescence detected in the spectral region used for Fig. 2B. Figs. 2A–D were captured in the same areas, as were the ROI lines. Figs. 2A and C are the main spectral images used to identify the AgNPs and GST, while Figs. 2B and D are the control images, which were captured outside of the emission spectra of the AgNPs and GST, respectively.

The plots of the ROIs indicated by 1, 2, and 3 reveal two fluorescence signals, while the ROIs indicated by 4, 5, and 6 reveal only a single signal, which is shown in red. The graphs of ROIs 1, 2, and 3 are representative of the images captured according to the first parameters, in which the spectral bands correspond to the highest fluorescence intensities of the GST and AgNPs, and therefore, both are present in the graphs. The plots of ROIs 1 and 2 show signs of co-location because the most intense fluorescence peaks are being emitted in the same location but with different intensities, which suggests the presence of both the AgNPs and GST at the selected points, *i.e.* the plots indicate the presence of GST-functionalized AgNPs. In the plot for ROI 3, there are overlapping fluorescence signals of nearly equal intensity, as shown by the red (AgNP-GST) and blue lines (AgNPs), which suggests that only free AgNPs have been being detected by the emission measurements of this ROI. This corresponds well with the signals observed in (Figure 2D). The plots for ROIs 4, 5, and 6 only contain one fluorescence signal in red. The blue line is not present because the chosen spectral range for Figures 2B and D was 380 to 440 nm, where the AgNPs do not emit fluorescence, as has been reported in the literature[24]. In addition, the signals represented by the red lines do not correspond to GST because GST does not emit fluorescence between 720 and 780 nm. Thus, the signals observed in (Figure 2D) correspond to the AgNPs, which fluoresce in this spectral region. Therefore, it is confirmed that under this second parameter only signals from AgNPs were detected. In addition, this data does not suggest the absence of GST on the surface of the AgNPs, but demonstrates that there are no overlapping signals, nor spectral interference between the AgNPs and GST, in this spectral region [1].

The 3D reconstruction (Figure 3A) indicates the presence of clusters of triangular nanoprisms, as reported in the literature for free AgNPs [26]. This pattern is highlighted in (Figure 3B), which corresponds to the demarcated area in (Figure 3A). Figure 3C shows that after the AgNPs have been functionalized, the GST is linked to the surface of the AgNPs, as indicated by the red colour surrounding the blue surfaces of the AgNPs. Thus, this image is evidence of the binding between the GST and AgNPs. In addition, the functionalization process used in this study provides AgNPs with the specific functionality to detect anti-GST.

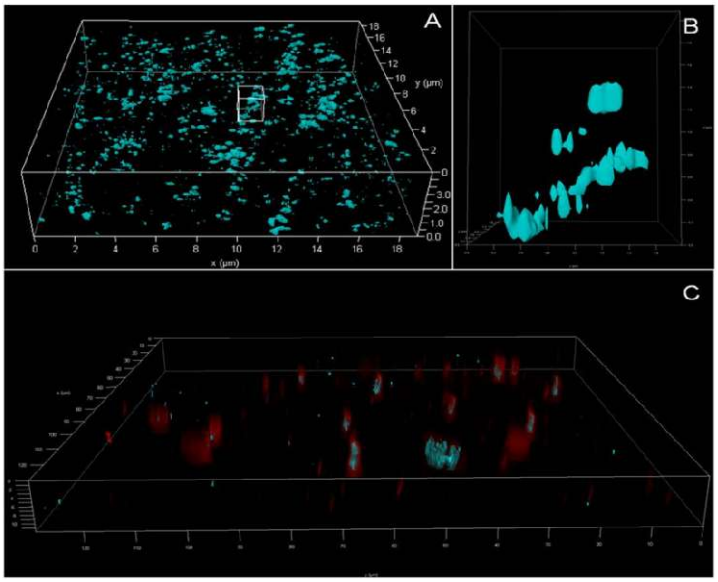

Figure 3. LSCM images of (A) free AgNPs and (B) a selected area, indicated by the box in (A), containing free AgNPs. (C) GST-functionalized AgNPs. The blue represents the AgNPs and the red represents the functionalized GST.

The nano-immunosensor activity of the AgNPs for detecting anti-GST was evaluated via spectroscopic techniques in the visible region (580 nm) of the electromagnetic spectrum. Figures 5A–F show the absorbance values of the immunoassays as a function of time. The absorbance was measured for a total of 60 min to ensure the complete precipitation of the immunoassay components, which is indicated by the complete discolouration of the suspension. The free-AgNP suspension is yellow, as shown in (Figure 4A). The suspension becomes orange when the GST

solution is added to the assay (Figure 4B), and adding the anti-GST solution to the GST-functionalized AgNPs makes the suspension become an intense orange colour (Figure 4C). These colour changes indicate the presence of molecular interactions between the GST-functionalized AgNPs and free anti-GST in the immunoassay. The surfaces of the AgNPs become sensitized to the intermolecular interactions via the functionalization process with GST, which enables the AgNPs to be used for the colorimetric biosensing of anti-GST biomolecules, that cause the colour of the immunoassay to change [27].

The antigen-antibody interaction is a specific chemical reaction that occurs via non-covalent bonds[28]. The interactions between the soluble antibodies and antigens results in the formation of a complex that is precipitated out of the suspension.

The precipitation rate of the complex depends on the relative quantities of antigens and antibodies present in the suspension. In typical experiments, to quantify this rate, the antibody concentration is kept constant and the antigen concentration is varied [29]. The purpose of this AgNP-based nano-immunosensor is to detect a specific antibody. Therefore, the GST concentration was maintained at 1000 ng/mL to functionalize the AgNPs and the GST-functionalized AgNP suspension was incubated with six solutions containing different concentrations of anti-GST. The first immunoassay was prepared with equivalent GST and anti-GST concentrations (1000 ng/mL).

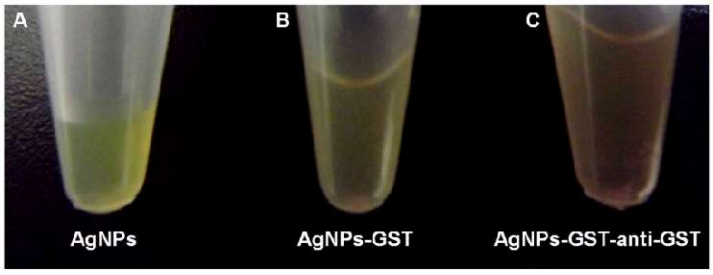

Figure 4. Photographs of the AgNP suspensions at various stages of the functionalization process. (A) Free AgNPs. (B) After adding GST to the AgNPs. (C) After adding anti-GST to the GST-functionalized AgNPs.

In this case, the optimum precipitation rate of the complex is achieved. In the antigen excess zone, or when there is a high level of antibody dilution, there is an insufficient concentration of antibodies to form and precipitate complexes, resulting in the formation of some soluble complexes that remain in the suspension[29]. By analysing Figs. 5A–F, it is concluded that the absorban ce values increase as the anti-GST concentration decreases. The 1:500 dilution (Figure 5A) results in the 100% formation of precipitates because the GST and anti-GST concentrations are equal (1000 ng/mL). In this case, the absorbance of the solution decreases as all of the GST molecules are released from the surface of the AgNPs and precipitate as complexes with the anti-GST molecules. On the other hand, with the more dilute immunoassays, there are fewer anti-GST molecules to interact with the GST and cause it to detach from the surface of the AgNPs, which results in increased absorption of such immunoassays [29]. In general, the absorbance decreases with increasing reaction time. Over the 60 min of reaction time, there was further precipitation of complexes. The destabilization of the AgNP suspension contributes to this precipitation because the experiments were performed at room temperature, which is not within the standard cooling temperatures needed to maintain the stability of the suspension. This issue is evidenced by the decreasing absorbance values as the reaction time increases (Figure 5).

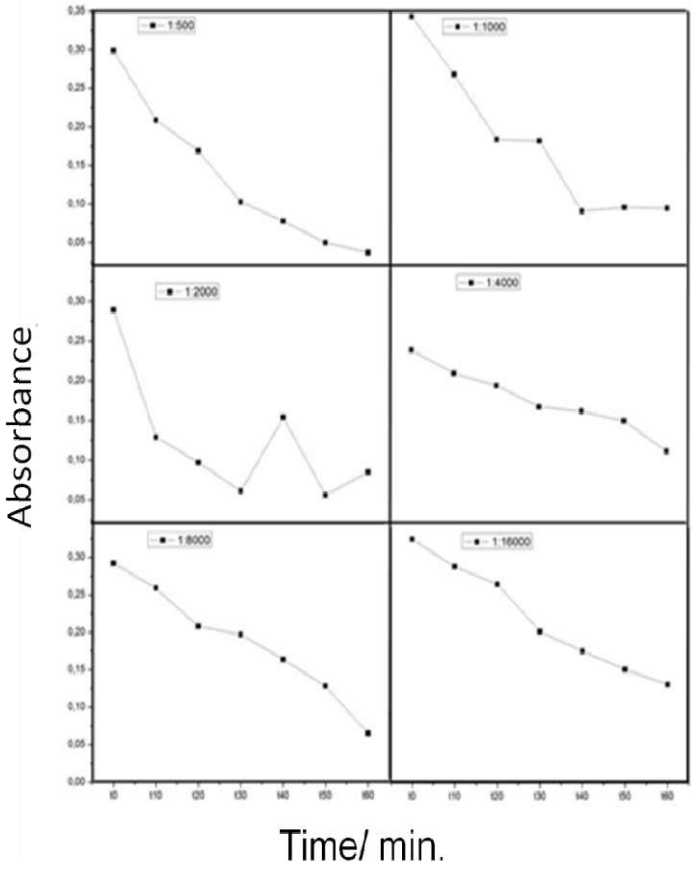

Figure 5. Plots showing the absorbance values of the immunoassays as a function of the reaction time in minutes for various anti-GST concentrations.

4. CONCLUSIONS

It is concluded that the synthesis of the AgNPs and functionalization process were effective, as evidenced by the topographic reconstructions created via LSCM and fluorescence intensity measurements that showed the co-location of the AgNPs and GST molecules. The interactions of the immunoassays composed of the GST-functionalized AgNPs and anti-GST molecules were verified by measuring the FT-IR spectra of the samples, which demonstrated the contribution of the antibody portion to the immunoassay. The sensing activity of the GST-functionalized AgNPs was monitored via spectrophotometric techniques, which allowed us to measure the detection of anti-GST as a function of the reaction time (60 min). It also enabled the monitoring of the room-temperature stability of the AgNP suspension.

Evidence of the success of the functionalization process and antibody detection was also possible with the naked eye, as the colour of the AgNP suspension changed when the biomolecules were added. We emphasize the significance of this result because it shows the potential of this AgNP-based nano-immunosensor to be applied as a diagnostic tool for autoimmune

diseases, such as multiple sclerosis, which does not have a specific biological marker. Thus, by emitting an optical signal, the AgNPs could be used as a non-invasive and low-cost diagnostic device for detecting the antibodies of a disease.

5. REFERENCES

[1]Shim S.-Y., Lim D.-K., Nam J.-M., Ultrasensitive optical biodiagnostic methods using metallic nanoparticles, *Nanomedicine (Lond)*, 3, 215–232, **2008.**

[2]Nair A. S., Tom R. T., Rajeev Kumar V. R., Subramaniam C., Pradeep T., Chemical Interactions At Noble Metal Nanoparticle Surfaces — Catalysis, Sensors and Devices, *Cosmos*, 3, 1,103–124, **2007.**

[3]Schroedter A., Weller H., Ligand design and bioconjugation of colloidal gold nanoparticles, *Angew. Chem. Int. Ed. Engl.*, 41, 17, 3218–21, **2002.**

[4]Hayes J. D., Flanagan J. U., Jowsey I. R., Glutathione transferases., *Annu. Rev. Pharmacol. Toxicol.*, 45, 51–88,**2005.**

[5]Knoblauch C., Griep M., Friedrich C., Recent advances in the field of bionanotechnology: an insight into optoelectric bacteriorhodopsin, quantum dots, and noble metal nanoclusters, *Sensors (Basel)*,14, 10,19731–66, **2014.**

[6]Mansur A., Mansur H., González J., Enzyme-polymers conjugated to quantum-dots for sensing applications., *Sensors (Basel)*, 11, 10, 9951–72, **2011.**

[7]Li Z., Lei Z., Zhang J., Liu D., Wang Z., Effects of Size, Shape, Surface Charge and Functionalization on Cytotoxicity of Gold Nanoparticles, *Nano Life*, 5, 1, 1540003, **2015**.

[8]Jamieson T., Bakhshi R., Petrova D., Pocock R., Imani M., Seifalian A. M., Biological applications of quantum dots, *Biomaterials*, 28, 31, 4717–32, **2007.**

[9]Xu K., Huang J., Ye Z., Ying Y., Li Y., Recent development of nano-materials used in DNA biosensors, *Sensors (Basel)*, 9, 5534–5557, **2009.**

[10]Zhong H., Bai Z., Zou B., Tuning the luminescence properties of colloidal I-II-VI semiconductor nanocrystals for optoelectronics and biotechnology applications, *J. Phys. Chem. Lett.*, 3, 3167–3175, **2012.**

[11]Tang L., Dong C., Ren J., Highly sensitive homogenous immunoassay of cancer biomarker using silver nanoparticles enhanced fluorescence correlation spectroscopy, *Talanta*, 81, 1560–1567, **2010.**

[12]Dawan S., Kanatharana P., Wongkittisuksa B., Limbut W., Numnuam A., Limsakul C., Thavarungkul P., Label-free capacitive immunosensors for ultra-trace detection based on the increase of immobilized antibodies on silver nanoparticles, *Anal. Chim. Acta*, 699, 232–241, **2011.**

[13]Chen L. Q., Xiao S. J., Peng L., Wu T., Ling J., Li Y. F., Huang C. Z., Aptamer-based silver nanoparticles used for intracellular protein imaging and single nanoparticle spectral analysis, *J. Phys. Chem. B*, 114, 3655–3659, **2010.**

[14]Naja G., Bouvrette P., Hrapovic S., Luong J. H. T., Raman-based detection of bacteria using silver nanoparticles conjugated with antibodies., *Analyst*, 132, 679–686, **2007.**

[15]Gorup L. F., Longo E., Leite E. R., Camargo E. R., Moderating effect of ammonia on particle growth and stability of quasi-monodisperse silver nanoparticles synthesized by the Turkevich method, *J. Colloid Interface Sci.*, 360, 2, 355–8, **2011.**

[16]Marangoni V. S., Paino I. M.,Zucolotto V., Synthesis and characterization of jacalin-gold nanoparticles conjugates as specific markers for cancer cells, *Colloids Surf. B. Biointerfaces*, 112, 380–6, **2013.**

[17]Ji J., Wang G., You X., Xu X., Functionalized silicon quantum dots by N-vinylcarbazole: synthesis and spectroscopic properties, *Nanoscale Res. Lett.*, 9, 1, 384–390, **2014.**

[18]Pillai Z. S., Kamat P. V, What factors control the size and shape of silver nanoparticles in the citrate ion reduction method?, *J. Phys. Chem. B*, 108, 945–951, **2004.**

[19]Tzvetkov N., Breuer P., Boteva R., Cysteine-free glutathione-S-tranferase as a tool for thiol-specific labeling of proteins, *Biotechniques*, 40, 145–146, **2006.**

[20]Ravindran A., Chandran P., Khan S. S., Biofunctionalized silver nanoparticles: Advances and prospects,*Colloids Surf. B Biointerfaces*, 105, 342–352, **2013.**

[21]Borase H. P., Patil C. D., Salunkhe R. B., Suryawanshi R. K., B. Kim S., Bapat V. A., Patil S. V., Bio-functionalized silver nanoparticles: A novel colorimetric probe for cysteine detection,*Appl. Biochem. Biotechnol.*, 175, 7, 3479–3493, **2015.**

[22]Saware K., Sawle B., Salimath B., Jayanthi K., Abbaraju V., Biosynthesis and characterization of silver nanoparticles using ficus benghalensis leaf extract, *International Journal of Research in Engineering and Technology*, **2014.**

[23]M. Gu, *Principles of Three Dimensional Imaging in Confocal Microscopes*. World Scientific, **1996.**

[24]Stranik O., Iacopino D., Nooney R., McDonagh C., Maccraith B. D., Optical properties of micro-patterned silver nanoparticle substrates., *J. Fluoresc.*, 20, 1, 215–23, **2010.**

[25]Manders E. M. M., Berbeek F. J., Aten J. A., Measurement of co-localization of objects in dual-colour confocal images, *J. Microsc.*, 169, 3, 375–382, **1993.**

[26]Milosavljevic V., Moulick A., Kopel P., Adam V., Kizek R., Micro wave preparation of carbon quantum dots with different surface modifi cation, *J. Met. Nanotechnologies*, 3, 16–22, **2014.**

[27]Gao X., Lu Y., He S., Li X., Chen W., Colorimetric detection of iron ions (III) based on the highly sensitive plasmonic response of the N-acetyl-L-cysteine-stabilized silver nanoparticles., *Anal. Chim. Acta*, 879, 118–125, **2015.**

[28]Janeway C. J., Travers P., Walport M., Shlomchik M. J., The interaction of the antibody molecule with specific antigen, in *Immunobiology: The Immune System in Health and Disease*, Garland Science, p. 600, **2001.**

[29]Doan T., Melvold R., Viselli S., Valtenbaugh C., *Immunology*. Lippincott Williams & Wilkins, **2012.**

6. ACKNOWLEDGEMENTS

We thank Miss Letícia Mariê Minatogau Ferro, MSc. Pâmela Soto Garcia and Rheabiotech Research and Development Laboratory for their kind support during the experimental stages of this work. We thank Dr. Leila Maria Beltramini for kindly providing the antigen and the antibody used in this work and for the helpful discussion and suggestions. We also thank the funding agencies National Council for Scientific and Technological Development (CNPq/INCT, 573742/2008–1), CAPES (PNPD/20131505), and FAPESP - São Paulo Research Foundation (FAPESP/CEPIDs, 13/07600–3) for their financial support of this work.